IEEE Photonics Journal
An IEEE Photonics Society Publication

A Tunable Optical Delay Line Based on Cascaded Silicon Nitride Microrings for Ka-Band Beamforming

Volume 11, Number 5, October 2019

Dongdong Lin
Xuemeng Xu
Pengfei Zheng
Huimin Yang
Guohua Hu
Binfeng Yun
Yiping Cui

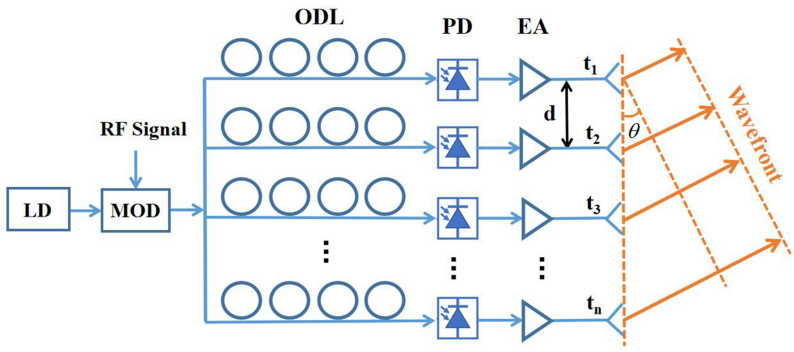

DOI: 10.1109/JPHOT.2019.2941510

A Tunable Optical Delay Line Based on Cascaded Silicon Nitride Microrings for Ka-Band Beamforming

Dongdong Lin, Xuemeng Xu, Pengfei Zheng, Huimin Yang, Guohua Hu, Binfeng Yun, and Yiping Cui

Advanced Photonics Center, Southeast University, Nanjing 210096, China

DOI:10.1109/JPHOT.2019.2941510

Manuscript received August 21, 2019; revised September 9, 2019; accepted September 11, 2019. Date of publication September 16, 2019; date of current version October 7, 2019. This work was supported in part by the National Key R&D Program of China under Grant 2018YFB2201800, in part by the National Science Foundation of Jiangsu Province under Grant BK 20161429, in part by the National Natural Science Foundation of China under Grant 61601118, and in part by the Postgraduate Research & Practice Innovation Program of Jiangsu Province under Grant KYCX19_0066. Corresponding author: B. Yun (e-mail: ybf@seu.edu.cn).

Abstract: A continuously tunable optical delay line with low delay ripple based on four cascaded tunable silicon nitride microring resonators for Ka-band beamforming network is proposed. The delay responses of the tunable optical delay line were investigated theoretically and experimentally. And a maximum delay tuning range of 300.3 ps, 169.4 ps and 88.6 ps were achieved when the delay bandwidth is set as 2 GHz, 5 GHz and 10 GHz respectively. In addition, low delay ripple about 8.5 ps and low additional loss less than 3.6 dB were obtained. Moreover, the maximum delay tuning range was increased to about 395 ps by combining the off-resonance region of the cascaded MRRs.

Index Terms: Optical delay line, microring resonator, microwave photonics.

1. Introduction

With the growth in wireless communication, the Ka-band (frequency ranges from 26.5 GHz to 40 GHz) has enormous potential for its wide bandwidth and compact antenna size. In the phased array antenna system, the beamforming technology can improve communication efficiency by transmitting and receiving microwave signals in a specific direction. However, for the traditional beamforming realized by the electrical phase shifters, beam squint [1] effect will be inevitable in wideband applications, since the electrical phase shifters are frequency correlative. The beam squint can be effectively avoided by replacing the electrical phase shifters with microwave photonics optical delay lines (ODLs), which have lower transmission loss, larger bandwidth, and immunity to electromagnetic interference [2], [3]. With the development of integrated microwave photonics, a variety of integrated ODLs have been proposed, such as photonic crystal waveguides [4], waveguide Bragg gratings [5], [6], optical switchable waveguides [7]–[9] and microring resonators (MRRs) [10]–[22]. Among them, the ODL structures based on optical switchable waveguides and tunable MRRs are relative simple and easy to fabricate. And both of them can be easily realized on the CMOS compatible platforms such as the silicon on insulator (SOI) and silicon nitride (Si_3N_4). In our previous work [9], we have realized a seven-bit ODL based on the optical switchable SOI waveguides, which is suitable for Ka-band beamforming. And the proposed ODL was designed with a delay increment

of 1.42 ps. However, the delay cannot be tuned continuously due to the fixed switchable waveguide lengths, which will limit the beam direction resolution. In order to realize continuous delay tuning, the MRR based ODLs with higher integration density have attracted a lot of researchers' interests.

In the MRR based ODL, the delay can be continuously tuned by adjusting the MRR's coupling coefficient. However, the delay bandwidth of a single MRR is very limited. In order to increase the delay bandwidth, off-resonance delay tuning method was proposed for single MRR [18], but only tens of picoseconds were realized. On the other hand, the delay tuning range can be increased by cascading more MRRs, which has a trade-off between delay tuning range, delay bandwidth, delay ripple, transmission loss and system complexity. As an example, a maximum delay of 135 ps was achieved by using cascaded SOI MRRs structure [14]. By combining the resonant and off-resonance regions of three cascaded Si_3N_4 MRRs, a 209 ps tuning range with bandwidth of 6 GHz was realized by precise tuning all the MRRs [20], to reduce the system complexity, binary tree structure was adopted to realize the 1×4 optical beamforming network (OBFN) in that work. However, in the binary tree structure, the two latter stages share the common MRR in the preceding stage, which cannot be tuned independently according to the two separate delay channels. So relative large delay ripple will occur, which will degrade wideband performance of the OBFN. In this paper, we proposed a continuously tunable ODL consisting of cascaded four Si_3N_4 MRRs, which can realize larger delay tuning range with larger delay bandwidth and smaller delay ripples. With every MRRs in the delay line can be tuned independently for different target delays, the delay ripples can be reduced to less than 10 ps compared with tens of ps of the binary tree structure. Here the Si_3N_4 waveguide was chosen to realize the ODL for the following reasons. First, as known, the double stripe Si_3N_4 waveguide we used has much lower refractive index contrast comparing with SOI waveguide, and lithography with much lower resolution was used to fabricate the MRRs. So no backscattering induced resonance splitting were observed in the fabricated Si_3N_4 MRRs [10]. Second, as known, the insertion loss of the ODL is extremely important for OBFN because the induced RF loss are doubled. Although the SOI waveguide has much larger thermo-optic coefficient comparing with Si_3N_4 waveguide, the double stripe Si_3N_4 waveguide we used has very low propagation loss of less than 0.2 dB/cm, which is one order lower than the typical propagation loss of 2∼3 dB/cm of SOI waveguide. In addition, only about 4 dB fiber to fiber coupling loss was achieved with the Si_3N_4 spot size converter, which is also much easier to achieve compared with the SOI waveguide. With the above merits, fiber to fiber insertion loss about 4 dB and additional loss less than 3.6 dB corresponding to the maximum delay were achieved, which is very difficult to obtained with the cascade SOI MRRs. Besides, the fabrication and packaging cost are much lower than the SOI MRRs.

2. Theory and Fabrication

Assume a one-dimensional optical controlled phased array antenna with n delay channels, as shown in Fig. 1, where each delay channel consists of four cascaded Si_3N_4 MRRs. The wavefront can be reconstructed to change the radiated beam direction by controlling the delay of each channel. In order to reduce the sidelobes of the beam, the distance between antennas is usually set as half wavelength of the transmitted radio frequency (RF) signal. Assume the RF frequency is 40 GHz, the distance between each antenna is:

$$d = \lambda/2 = 3 \times 10^8 / \left(2 \times 40 \times 10^9\right) m = 0.00375 \text{ m} = 3.75 \text{ mm} \tag{1}$$

To achieve a scan angle of $-60°\sim60°$, the maximum delay between adjacent channels is:

$$\Delta t_{\max} = \frac{2 \times d \cdot \sin 60}{c} \approx \frac{2 \times 0.00375 \times 0.866}{3 \times 10^{11}} s \approx 21.65 \text{ ps} \tag{2}$$

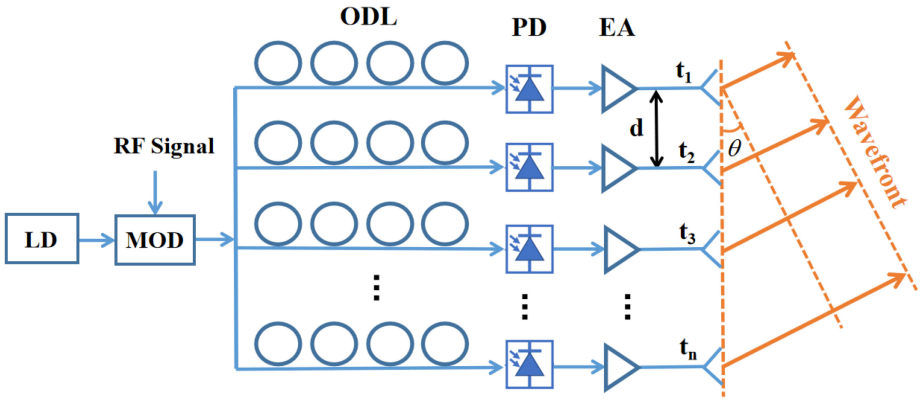

Fig. 1. The schematic diagram of optical controlled phased array antenna with 1 × n OBFN. LD: laser diode, MOD: modulator, ODL: optical delay line, PD: photodetector, EA: Electrical amplifier.

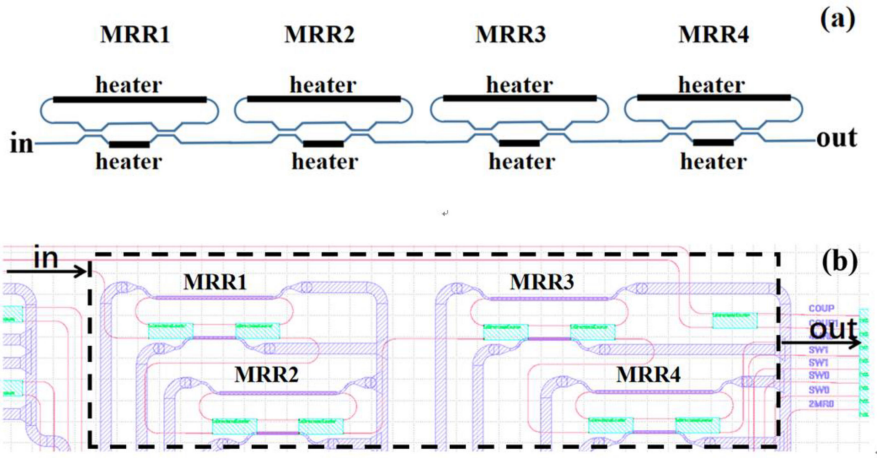

Fig. 2. (a) The schematic diagram of designed ODL. (b) The mask layout of designed ODL.

Therefore, the maximum delay between the 1st and nth channels with angle scan range of −60°∼60° is:

$$\Delta T_{\max} = 21.65 * (n - 1) \tag{3}$$

It can be seen that an ODL with minimum delay tuning range of ΔT_{max} is needed for a 1 × n OBFN working at 40 GHz to achieve angle scan range of −60°∼60°.

The schematic diagram of the proposed four cascaded MRRs (4-MRRs) is shown in Fig. 2(a), where the mask layout is shown in Fig. 2(b). Tunable Mach-Zehnder interferometer (MZI) coupled MRR was chosen as the building block of the 4-MRRs. And a double stripe Si_3N_4 waveguide with propagation loss less than 0.2 dB/cm was used to achieve high quality factor [23], which can increase the maximum delay. The bending radius of the MRRs were designed as 125 um to ensure that the bending loss is low enough to be neglected. And the roundtrip length of the MRR is about 3350 um, which corresponds to a FSR about 50 GHz. In addition, each tunable MRR has two heaters with lengths of 400 um and 1100 um for adjusting the coupling coefficient and resonant frequency, respectively. The chip size of the designed 4-MRRs is about 6400 um × 2000 um.

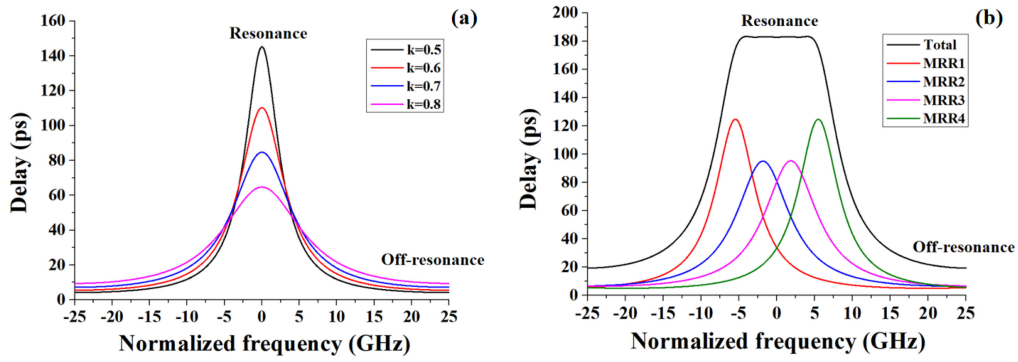

Fig. 3. (a) Single MRR delay spectra for different values of k. (b) The typical flattened delay spectrum of the 4-MRRs and the corresponding delays of the four individual MRRs.

The transfer function of the tunable MZI coupled MRR can be obtained using the transfer matrix method, which can be expressed as [24]:

$$H_n(\omega) = \frac{\sqrt{1-k_n} - \alpha \cdot e^{j(\varphi_n(\omega)+\phi_n)}}{1-\sqrt{1-k_n}\cdot\alpha\cdot e^{j(\varphi_n(\omega)+\phi_n)}} \tag{4}$$

Where k_n ($n = 1 \sim 4$) is the power cross coupling coefficient of the tunable MZI, α represents the round trip loss coefficient of the MRR, $\varphi_n(\omega)$ ($n = 1 \sim 4$) represents the round trip phase shift of the MRR, ϕ_n ($n = 1 \sim 4$) represents the additional phase shift introduced by the heater on the MRR. Therefore, by multiply the transfer functions of the four cascaded MRRs, the transfer function of the proposed 4-MRRs can be expressed as:

$$H_{delay}(\omega) = H_1(\omega)\cdot H_2(\omega)\cdot H_3(\omega)\cdot H_4(\omega) \tag{5}$$

Then, the delay spectrum of the 4-MRRs can be obtained by the phase spectrum differentiation:

$$T(\omega) = -\frac{d\left(\Psi\left(H_{delay}(\omega)\right)\right)}{d(\omega)} \tag{6}$$

Where $\Psi(H_{delay}(\omega))$ is the phase response of the 4-MRRs, ω is the angular frequency.

For a single MRR, the group delay is related to the power cross coupling coefficient k according to Eq. (4) and Eq. (6). The quality factor of the MRR is decreased when increasing k because the light can be much easier to escape from the ring cavity. In other words, the group delay is decreased with increasing k. However, the delay bandwidth can be enlarged due to the decreased quality factor. Here we simulated the group delay spectra of the single Si_3N_4 MRR with different k as shown in Fig. 3(a). It is obvious that the group delay can be increased by decreasing k. However, the obtained group delay and delay bandwidth of the single Si_3N_4 MRR is not enough for wideband operation, since there is an intrinsic trade-off between the group delay and the delay bandwidth. Here four cascade MRRs are introduced to balance the group dealy and the delay bandwidth based on the group delay spectra overlay of four cascade Si_3N_4 MRRs. In order to get a flat and wideband group delay spectrum, the resonant frequencies and the power cross coupling coefficients of the four Si_3N_4 MRRs should be adjusted properly as shown in Fig. 3(b). And by using the thermo-optic effect, the resonant frequencies and the power cross coupling coefficient can be adjusted by the heaters in the ring and the MZI region, respectively. Through carefully adjusting the coupling coefficient and the resonant frequency of each MRR, a typical flattened delay spectrum can be obtained as shown in Fig. 3(b). Here α is set as 0.9797, and the coupling coefficients of the 4-MRRs are set as $k_1 = 0.55458$, $k_2 = 0.65584$, $k_3 = 0.65584$, $k_4 = 0.55458$ respectively. The additional phase shifts of $\phi_1 = -0.67885$ rad, $\phi_2 = -0.22845$ rad, $\phi_3 = 0.22845$ rad and $\phi_4 = 0.67885$ rad were introduced to achieve suitable resonant frequencies of the 4-MRRs, respectively. And with above optimization, a total delay about 182.9 ps with 10 GHz delay bandwidth and delay ripples of 0.5 ps are obtained.

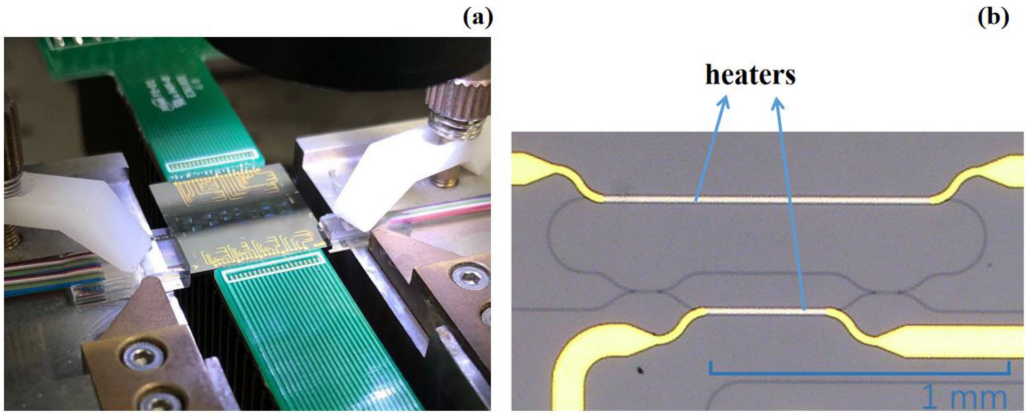

Fig. 4. (a) The packaged chip on the designed PCB. (b) The optical microscope image of MRR in the fabricated chip.

The 4-MRRs ODL chip was fabricated in LioniX International using TriPleX ADS technology, which is based on a low loss double stripe Si_3N_4 waveguide realized on 100 mm silicon wafers with 8 μm thermal oxide [26]. The propagation loss of the fabricated waveguide is about 0.12 dB/cm according to our measurements with the cutback method. Fig. 4(a) shows the packaged chip wire bonded to a customized PCB, and the measured input/output coupling loss between the chip and fiber array is about 4 dB by adopting the provided spot size converter. Fig. 4(b) shows the optical microscope image of the MRR in the fabricated chip.

3. Results and Discussion

The transmission and delay spectra of the proposed 4-MRRs were measured by the lightwave measurement system (LMS, Agilent 8164A) and the optical vector network analysis (OVNA) method, respectively. By scanning the tunable laser wavelength in LMS, the transmission spectrum of the 4-MRRs can be easily obtained. And the OVNA measurement system based on the optical single sideband (OSSB) modulation [25] is shown in Fig. 5. Where the laser from a tunable laser source (Santac WSL-100) with output power of 15 dBm was injected into the Mach-Zehnder modulator (EOSpace AX-0MSS-20-PFA-PFA-LV). The modulator working at the quadrature bias was driven by the RF signals from the vector network analyzer (Agilent N5242A) and the optical double sideband modulation (ODSB) was obtained. Then, an optical tunable filter (Santac OTF-980) was used to tailor one optical sideband to get the OSSB modulation. And a photodetector (Finisar XPDV2120RA) was adopted to retrieve the RF output signal, which was sent back to the vector network analyzer to obtain the delay spectrum. Due to the maximum frequency sweeping range of 26.5 GHz of our vector network analyzer, which is smaller than the measurement range required for the proposed 4-MRRs, the delay spectrum measurement was divided into three parts and each has a frequency sweeping range of 15 GHz. Finally, the total delay spectrum of the 4-MRRs was obtained by changing the laser carrier wavelength and stitch the obtained three individual delay spectra.

By carefully adjusting the driving voltages of all the eight heaters of the 4-MRRs, relatively flattened delay responses of the designed ODL and the corresponding transmission spectra were measured by using the OVNA method and the LMS, respectively. And according to Eq. 4–Eq. 6, the measured flattened transmission and delay spectra of the ODL were fitted by adjusting the coupling coefficient and resonant frequency of each MRR, the fitted cross coupling coefficients of the 4-MRRs are shown in Table 1, the obtained results are shown in Fig. 6 and Fig. 7, where the points and the solid curves denote the normalized measured and simulated spectra, respectively. We can see that the measured results match the simulation very well. The insertion loss variation range of the fabricated ODL is about 4 dB$\sim$7.5 dB during the delay tuning. A delay tuning range

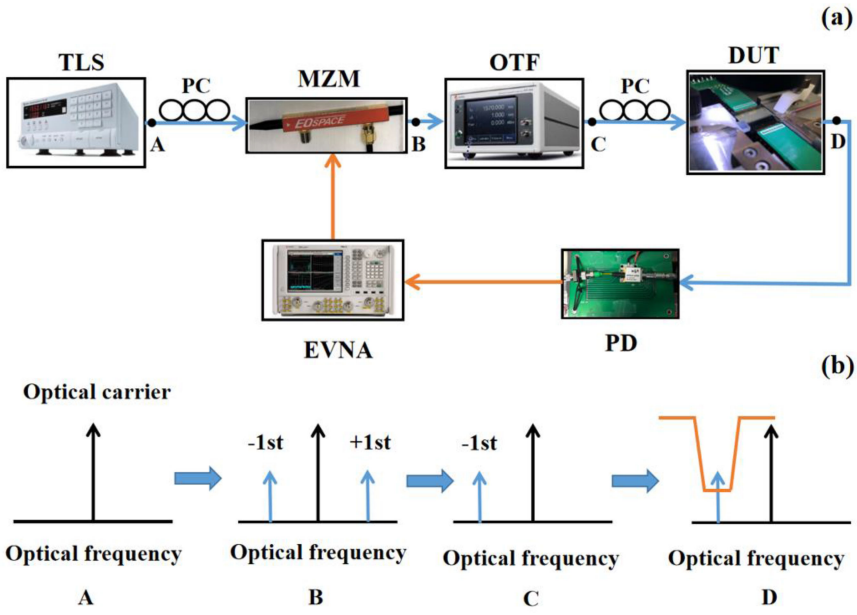

Fig. 5. (a) The experimental setup of delay test based OVNA link. TSL: tunable laser source, PC: polarization controller, MZM: Mach-Zehnder modulator, OTF: optical tunable filter, DUT: device under test, PD: photodetector, EVNA: electronics vector network analyzer. (b) The principle diagram of the OSSB in the frequency domain.

TABLE 1

The Fitted Cross Coupling Coefficients k_n of the 4-MRRs of the Four Typical Delay Spectra

Normalized transmission (dB)	Delay (ps)	Bandwidth (GHz)	k_1	k_2	k_3	k_4
-0.85	94.3	16	0.857	0.921	0.921	0.857
-1.65	182.9	10	0.555	0.656	0.656	0.555
-2.38	263.7	5	0.440	0.540	0.540	0.440
-3.56	394.6	2	0.390	0.518	0.518	0.390

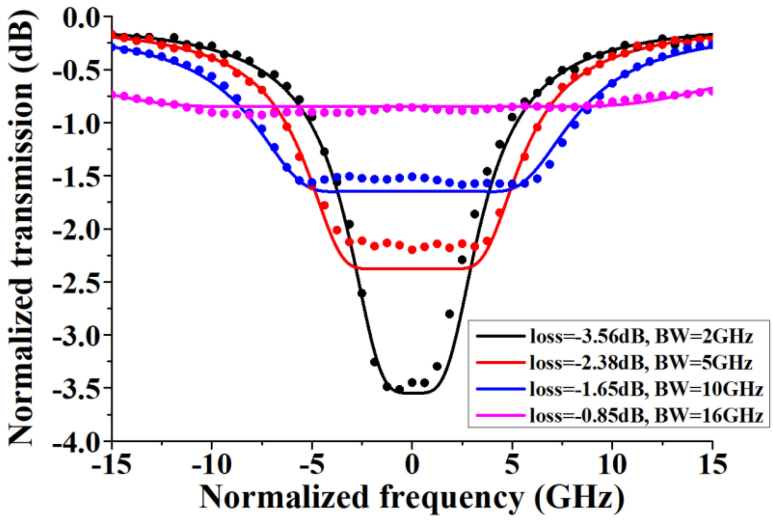

Fig. 6. Simulated and measured transmission spectra.

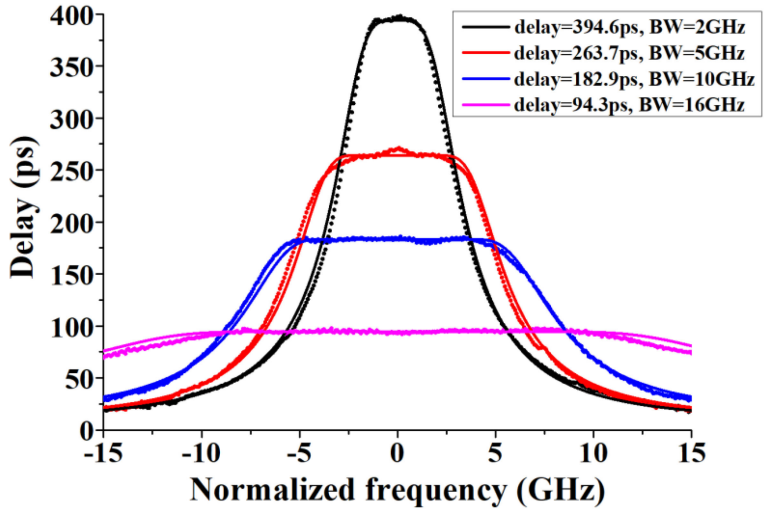

Fig. 7. Simulated and measured delay spectra.

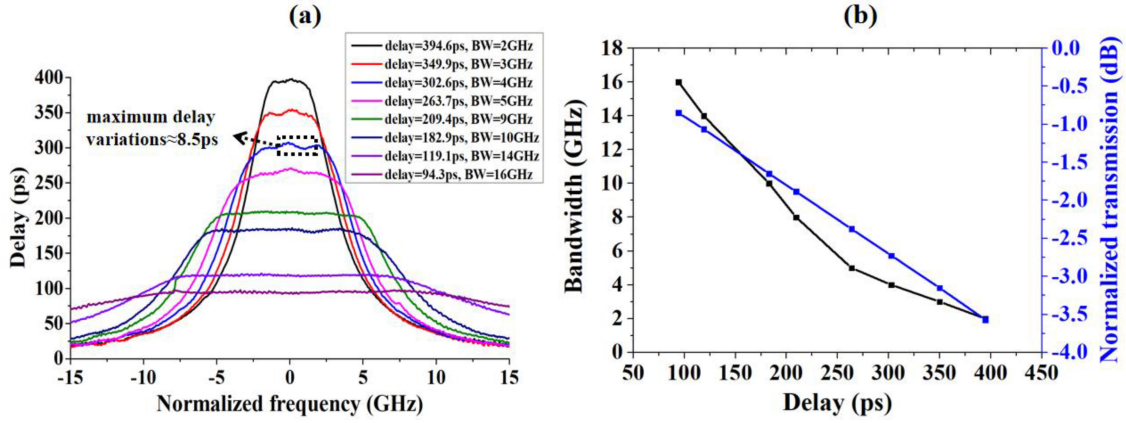

Fig. 8. (a) Measured delay spectra. (b) The relationships between delay, bandwidth and normalized transmission.

from 94.3 ps to 394.6 ps with 2 GHz bandwidth was obtained in the resonant region. In other words, a maximum delay tuning range of 300.3 ps with 2 GHz bandwidth was achieved, while the normalized transmission is only varied from 0.85 dB to 3.56 dB.

More delay spectra measurement results are shown in Fig. 8(a) and the relationships between the delay, bandwidth and normalized transmission are shown in Fig. 8(b). It is obvious that there is a trade-off between the delay tuning range and the delay bandwidth. As we can see, a 300.3 ps delay tuning range with bandwidth of 2 GHz, or a 169.4 ps delay tuning range with bandwidth of 5 GHz, or a 88.6 ps delay tuning range with bandwidth of 10 GHz were obtained. And maximum channel numbers of 14, 8 and 4 can be supported for the OBFN working at 40 GHz with $-60°\sim60°$ angle scan range as shown in Table 2. Moreover, the measured maximum delay ripples in working frequency band is only about 8.5 ps.

The above delay measurement results were obtained at the resonant region of the cascaded MRRs. In addition, a larger delay tuning range can be achieved by leading into the off-resonance region of the cascaded MRRs [20], [21], as shown in Fig. 9, where the two measured delay spectra at the bottom were obtained in the off-resonance region of the cascaded MRRs. So with the off-

TABLE 2
The Relationships Between Delay Tuning Range, Bandwidth and Maximum Supported Channel Number

Delay tuning range (ps)	Bandwidth (GHz)	Maximum supported channel number
300.3	2	1×14
169.4	5	1×8
88.6	10	1×4

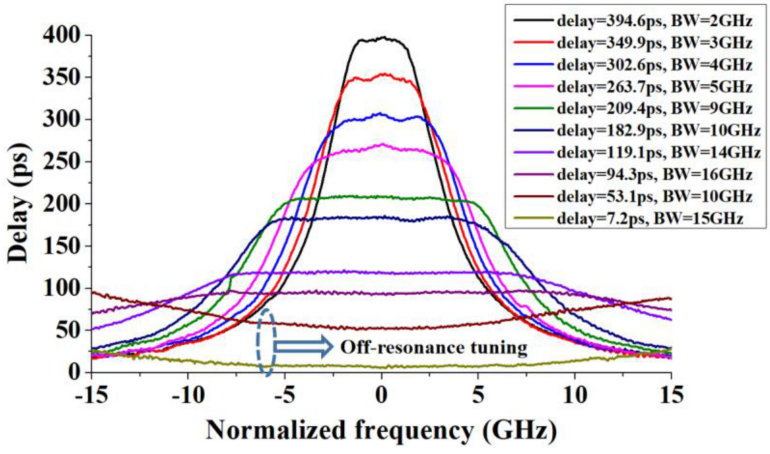

Fig. 9. Measured delay spectra with resonance and off-resonance of the cascaded MRRs.

TABLE 3
The Performance Comparison Between our ODL and Other MRR Based ODLs

	This work	Ref [22]	Ref [20]
Integration platform	Si_3N_4	SOI	Si_3N_4
Maximum number of MRRs per channel	4	3	3
FSR	50 GHz	50 GHz	22 GHz
Maximum delay tuning range @ bandwidth	394.6 ps @ 2 GHz 209.4 ps @ 9 GHz	164 ps @ 2 GHz	209 ps @ 6 GHz
Maximum Delay ripples	0.5 ps in theory ~8.5 ps in experiments	1.6 ps in theory /	2.32 ps in theory ~16 ps in experiments

resonance region, we can get a delay tuning range from 0 ps to 394.6 ps with 2 GHz bandwidth theoretically. And the performance comparison between our and other MRR based ODLs in the previous reports is shown in Table 3. Compared to Ref [22], by using the Si_3N_4 waveguide with lower propagation loss about 0.2 dB/cm and lower input/output coupling loss of about 4 dB, lower insertion loss is obtained. Also much larger delay tuning range is achieved with more cascade MRRs. Compared to Ref [20], with the same delay tuning range of 209 ps, the delay bandwidth is 50 percent larger, and the delay ripples are much smaller due to more MRRs are used in our work. In addition, the FSR of our designed MRR is increased to 50 GHz, which is better for wideband applications. We also compared the performances of our ODL with other ODLs with different structures, as shown in Table 4. Compared to Ref [11], larger delay tuning range is achieved in our work, a relative larger bandwidth was obtained by using coupled-resonator optical waveguides

TABLE 4
The Performance Comparison Between our ODL and Other ODLs With Different Structures

	This work	Ref [11]	Ref [5]	Ref [9]
Integration platform	Si_3N_4	Polymers	SOI	SOI
Structure	Cascaded MRRs (SCISSORs)	Cascaded MRRs (CROWs)	Waveguide Bragg gratings	Switchable waveguides
Maximum delay tuning range @ bandwidth	394.6 ps @ 2 GHz 209.4 ps @ 9 GHz	140 ps @>17GHz	25.7 ps @>8GHz	180.34 ps (7 bit)
Tuning method	Continuous	Continuous	Continuous	Discrete

(CROWs) with twelve coupled MRRs, which made it very difficult to tune due to the coupling between the MRRs. And the side-coupled integrated spaced sequence of resonators (SCISSORs) structure used in our work shows more tolerances to the manufacturing variation than the CROWs structure. Compared to Ref [5], much larger delay tuning range is achieved in our work with larger bandwidth, and cascaded MRRs are relative simple and easy to fabricate compared to waveguide Bragg gratings. Compared to Ref [9], larger delay tuning range is achieved in this work, although the bandwidth of switchable waveguides should be much larger than cascaded MRRs, only discrete delay can be switched, which will limit the beam direction resolution.

4. Conclusion

We proposed a continuously tunable ODL for Ka-band OBFN, the ODL consists of four cascaded tunable Si_3N_4 MRRs. And the ODL can realize delay tuning range of 300.3 ps, 169.4 ps and 88.6 ps when the delay bandwidth is set as 2 GHz, 5 GHz and 10 GHz respectively. With these delay settings, maximum channel numbers of 14, 8 and 4 can be supported for the OBFN working at 40 GHz with $-60°\sim60°$ angle scan range. Also a larger delay tuning range about 395 ps can be obtained by combining off-resonance region of the cascaded MRRs. In our future work, beamforming and data transmission experiments at Ka-band will be performed based on this ODL chip.

References

[1] I. Frigyes and A. J. Seeds, "Optically generated true-time delay in phased array antennas," *IEEE Trans. Microw. Theory Techn.*, vol. 43, no. 9, pp. 2378–2386, Sep. 1995.
[2] J. Capmany and D. Novak, "Microwave photonics combines two worlds," *Nat. Photon.*, vol. 1, no. 6, pp. 319–330, 2007.
[3] J. Yao, "Microwave photonics," *J. Lightw. Technol.*, vol. 27, no. 3, pp. 314–335, 2009.
[4] J. Sancho *et al.*, "Integrable microwave filter based on a photonic crystal delay line," *Nat. Commun.*, vol. 3, 2012, Art. no. 1075.
[5] M. Burla, L. Cortés, M. Li, X. Wang, L. Chrostowski, and J. Azaña, "Integrated waveguide Bragg gratings for microwave photonics signal processing," *Opt. Exp.*, vol. 21, no. 21, pp. 25120–25147, 2013.
[6] J. Wang *et al.*, "Subwavelength grating enabled on-chip ultra-compact optical true time delay line," *Sci. Rep.*, vol. 6, no. 1, 2016, Art. no. 30235.
[7] J. Xie, L. Zhou, Z. Li, J. Wang, and J. Chen, "Seven-bit reconfigurable optical true time delay line based on silicon integration," *Opt. Exp.*, vol. 22, no. 19, pp. 22707–22715, 2014.
[8] S. Fathpour and N. A. Riza, "Silicon-photonics-based wideband radar beamforming: basic design," *Opt. Eng.*, vol. 49, no. 1, 2010, Art. no. 018201.
[9] P. Zheng *et al.*, "A Seven bit silicon optical true time delay line for Ka-band phased array antenna," *IEEE Photon. J.*, vol. 11, no. 4, Aug. 2019, Art. no. 5501809.
[10] A. Li, T. V. Vaerenbergh, P. D. Heyn, P. Bienstman, and W. Bogaerts, "Backscattering in silicon microring resonators: A quantitative analysis," *Laser Photon. Rev.*, vol. 10, no. 3, pp. 420–431, 2016.
[11] J. K. S. Poon, L. Zhu, G. A. De Rose, and A. Yariv, "Transmission and group delay of microring coupledresonator optical waveguides," *Opt. Lett.*, vol. 31, no. 4, pp. 456–458, 2006.
[12] L. Zhuang, C. Roeloffzen, R. Heideman, A. Borreman, A. Meijerink, and W. van Etten, "Single-chip ring resonator-based 1×8 optical beam forming network in CMOS-compatible waveguide technology," *IEEE Photon. Technol. Lett.*, vol. 19, no. 15, pp. 1130–1132, Aug. 1 2007.

[13] L. Zhuang *et al.*, "Novel ring resonator-based integrated photonic beamformer for broadband phased array receive antennas—Part II: Experimental prototype," *J. Lightw. Technol.*, vol. 28, no. 1, pp. 19–31, Jan. 2010.
[14] J. Cardenas *et al.*, "Wide-bandwidth continuously tunable optical delay line using silicon microring resonators," *Opt. Exp.*, vol. 18, no. 25, pp. 26525–26534, 2010.
[15] M. Burla *et al.*, "Integrated photonic K_u-band beamformer chip with continuous amplitude and delay control," *IEEE Photon. Technol. Lett.*, vol. 25, no. 12, pp. 1145–1148, Jun. 2013.
[16] J. Xie, L. Zhou, Z. Zou, J. Wang, X. Li, and J. Chen, "Continuously tunable reflective-type optical delay lines using microring resonators," *Opt. Exp.*, vol. 22, no. 1, pp. 817–823, 2014.
[17] C. Xiang, M. Davenport, J. Khurgin, P. Morton, and J. Bowers, "low-loss continuously tunable optical true time delay based on Si3N4 ring resonators," *IEEE J. Sel. Top. Quantum Electron.*, vol. 24, no. 4, Jul.-Aug. 2018, Art. no. 5900109.
[18] N. Tessema *et al.*, "Wavelength-dependent continuous delay based on a Si3N4 optical ring resonator for K-band radio beamformer," in *Proc. IEEE Int. Topical Meeting Microw. Photon.*, 2016, pp. 305–308.
[19] N. Tessema *et al.*, "A tunable Si3N4 integrated true time delay circuit for optically-controlled K-band radio beamformer in satellite communication," *J. Lightw. Technol.*, vol. 34, no. 20, pp. 4736–4743, Oct. 2016.
[20] Y. Liu *et al.*, "Tuning optimization of ring resonator delays for integrated optical beam forming networks," *J. Lightw. Technol.*, vol. 35, no. 22, pp. 4954–4960, Nov. 2017.
[21] Y. Liu *et al.*, "Ultra-low-loss silicon nitride optical beamforming network for wideband wireless applications," *IEEE J. Sel. Top. Quantum Electron.*, vol. 24, no. 4, Jul.-Aug. 2018, Art. no. 8300410.
[22] G. Choo, C. Madsen, S. Palermo, and K. Entesari, "Automatic monitor-based tuning of an RF silicon photonic 1×4 asymmetric binary tree true-time-delay beamforming network," *J. Lightw. Technol.*, vol. 36, no. 22, pp. 5263–5275, Nov. 2018.
[23] R. G. Heideman, A. Leinse, M. Hoekman, F. Schreuder, and F. H. Falke, "TriPleX TM: The low loss passive photonics platform: Industrial applications through multi project wafer runs," in *Proc. IEEE Photon. Conf.*, Dec. 2014, pp. 224–225.
[24] C. C. Katsidis and D. I. Siapkas, "General transfer-matrix method for optical multilayer systems with coherent, partially coherent, and incoherent interference," *Appl. Opt.*, vol. 41, no. 19, pp. 3978–3987, 2002.
[25] S. Pan and M. Xue, "Ultrahigh-resolution optical vector analysis based on optical single-sideband modulation," *J. Lightw. Technol.*, vol. 35, no. 4, pp. 836–845, Feb. 2017.
[26] Lionix International, [Online]. Available: https://photonics.lionix-international.com